
CrossGET: Cross-Guided Ensemble of Tokens for Accelerating Vision-Language Transformers

Dachuan Shi^{1,2} Chaofan Tao³ Anyi Rao⁴ Zhendong Yang¹ Chun Yuan^{1*} Jiaqi Wang^{2*}
¹Tsinghua University ²Shanghai AI Laboratory ³The University of Hong Kong ⁴Stanford University
{sdc21@mails, yangzd21@mails, yuanc@sz}.tsinghua.edu.cn cftao@connect.hku.hk
anyirao@stanford.edu wangjiaqi@pjlab.org.cn

Abstract

Vision-language models have achieved tremendous progress far beyond what we ever expected. However, their computational costs and latency are also dramatically growing with rapid development, making model acceleration exceedingly critical for researchers with limited resources and consumers with low-end devices. Although extensively studied for unimodal models, the acceleration for multimodal models, especially the vision-language Transformers, is still relatively under-explored. Accordingly, this paper proposes **Cross-Guided Ensemble of Tokens (CrossGET)** as a universal vision-language Transformer acceleration framework, which adaptively reduces token numbers during inference via cross-modal guidance on-the-fly, leading to significant model acceleration while keeping high performance. Specifically, the proposed *CrossGET* has two key designs: 1) *Cross-Guided Matching and Ensemble*. *CrossGET* incorporates cross-modal guided token matching and ensemble to merge tokens effectively, only introducing cross-modal tokens with negligible extra parameters. 2) *Complete-Graph Soft Matching*. In contrast to the previous bipartite soft matching approach, *CrossGET* introduces an efficient and effective complete-graph soft matching policy to achieve more reliable token-matching results. Extensive experiments on various vision-language tasks, datasets, and model architectures demonstrate the effectiveness and versatility of the proposed *CrossGET* framework. The code will be at github.com/sdc17/CrossGET.

1 Introduction

The AI community is now witnessing the bloom of vision-language models [32, 27, 3, 61, 66, 21, 50, 62, 38, 37, 48, 43], among which transformer-based models such as CLIP [50], BLIP [38], and GPT-4 [48] have become dominant in recent studies. These models can tackle a broad range of vision-language tasks, such as Image-Text Retrieval [23], Vision Reasoning [57], Image Caption [42], and Visual Question Answer (VQA) [3]. Nevertheless, the notable improvement in model performance is at the expense of significantly increased computational cost. As a result, high computational requirements and unbearable latency are now preventing researchers with limited resources and consumers with low-end devices from enjoying the advances of these vision-language Transformers.

For accelerating deep models, there are already plenty of representative approaches, including but not limited to token reduction [6, 51, 56, 5, 41, 67, 4], model pruning [14, 16, 8, 46, 72, 5], quantization [64, 59, 10, 70, 11], and knowledge distillation [17, 71, 24, 63, 60, 65]. Although these methodologies are widely studied on unimodal models, there still exists a broad space in multimodal scenarios, *e.g.*, accelerating vision-language Transformers. A few works have tried it by model pruning [54] or knowledge distillation [9]. However, these existing approaches mainly focus on reducing the parameters of models and usually yield less speedup than token reduction.

*Corresponding authors.

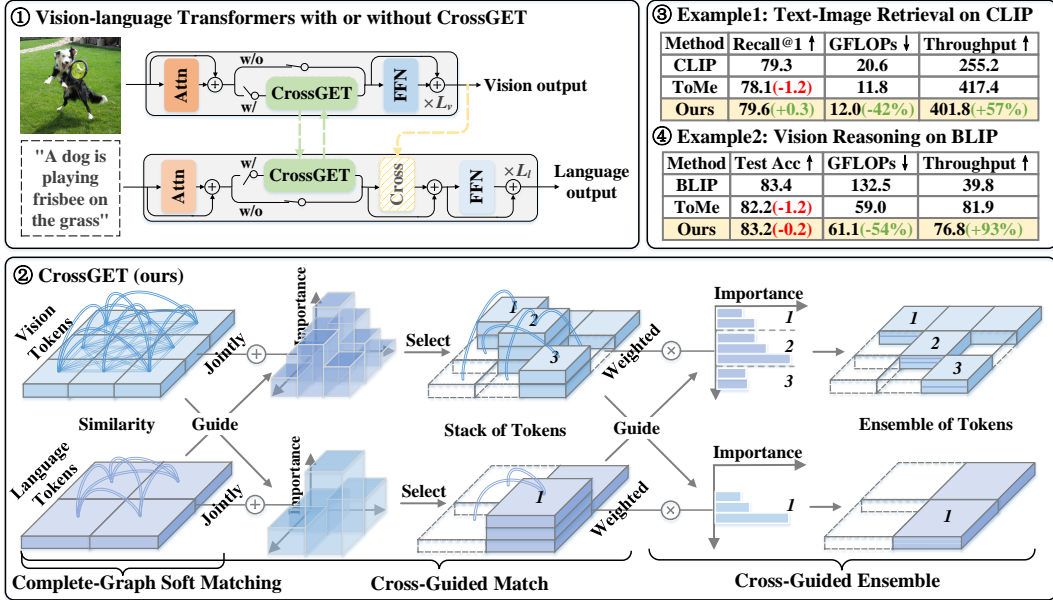


Figure 1: Overview of *CrossGET*. (1) *CrossGET* is a universal multimodal token reduction framework that can be applied to both modality-independent models (e.g., CLIP [50]) and modality-dependent models (e.g., BLIP [38]). (2) *CrossGET* jointly consider the token similarity given by intra-modal complete-graph soft matching and token importance given by cross-modal guidance to determine which tokens should be stacked together. And the cross-modal importance will be used again to weight tokens within each stack to output their ensembles. (3) and (4) The \uparrow and \downarrow indicate the higher the better and the lower the better, respectively. The unit of throughput is image-text pairs per second. Compared to original models, *CrossGET* achieves considerable computation saving and acceleration with negligible performance degradation (sometimes even get improvements); *CrossGET* also outperforms the SOTA token reduction approach ToMe [4] in various multimodal scenarios.

Accordingly, this paper introduces *CrossGET* as a novel token reduction method for vision-language Transformers, which speeds up model inference via adaptively reducing the number of tokens on-the-fly. Considering the major challenge of designing a token reduction method is to determine and eliminate redundant tokens, *CrossGET* introduces two key designs for accelerating vision-language Transformers, i.e., *cross-guided matching and ensemble* and *complete-graph soft matching*.

First, *CrossGET* introduces *cross-guided matching and ensemble* to determine and merge redundant tokens for both modality-independent models (e.g., CLIP [50]) and modality-dependent models (e.g., BLIP [38]). Precisely, *CrossGET* injects cross tokens with negligible parameters into both vision and language branches, letting them learn cross-modal importance and guide the selection of redundant tokens.² Moreover, the cross-modal importance also serves as the guidance to merge tokens in a weighted ensemble manner.

Second, the previous work adopts a bipartite soft matching approach [4], which splits tokens into two sets alternately, leading to a suboptimal token assignment. *CrossGET* proposes an efficient and effective *complete-graph soft matching* to align similar tokens in a fully-connected graph, achieving more reliable token-matching results.

CrossGET's contributions can be summarized as

- It is one of the early works on token ensemble framework dedicated to vision-language Transformers acceleration, achieving a better performance-efficiency trade-off with negligible extra parameters.
- It proposes *cross-guided matching and ensemble* to exploit cross-modal information effectively and *complete-graph soft matching* for more reliable token-matching.

²A naive solution is directly calculating the similarity between vision and language tokens. However, in the modality-dependent model, e.g., BLIP-NLVR [38], the first layer of the language branch requires the last layer's output of the vision branch as its input. The cross-modal similarity is not available for the vision branch. Cross tokens in *CrossGET* serve as agents for other modalities, providing cross-modal guidance free from inference.

- Its framework’s effectiveness and versatility are validated by thorough experiments conducted on various vision-language tasks, datasets, and model architectures.

2 Related Work

Vision-Language Transformers According to dependency on the computation order of different modalities, the existing vision-language Transformers can be summarized into two categories: 1) modality-independent models [40, 39, 50, 31, 55]. for example CLIP [50] is a representative model. Specifically, it is feasible first to compute the visual or language branches. 2) modality-dependent models[39, 69, 38, 2, 37], for example BLIP-NLVR [38] is a representative model. Specifically, it is only feasible to compute the vision branch first. *CrossGET* is designed to be a universal framework that can be used for both modality-independent and modality-dependent models.

Token Reduction Some prior works have made progress in unimodal scenarios, for example, token reduction for vision scenarios [6, 51, 56, 5, 41, 67, 4] or language scenarios [12, 29, 30, 35]. To the best of our knowledge, *CrossGET* is the first token reduction framework dedicated to multimodal scenarios. It is also one of the few approaches that do not require any additional learnable parameters other than negligible cross tokens. And the most similar work to *CrossGET* from this point of view is the unimodal approach ToMe [4]. In addition to the proposed *cross-guided matching and ensemble* specifically for multimodal scenarios, *CrossGET* also proposes an improved *complete-graph soft matching* which is different from the *bipartite soft match* adopted by ToMe.

Multimodal Transformer Acceleration There are only a few works have attempted to accelerate multimodal Transformers. For example, DistillVLM [9] suggests that small vision-language models can use knowledge distillation to mimic the attention distribution of large ones. And UPop [54] proposes that small vision-language models can be unifiedly searched in large ones and then progressively pruned from the large ones. The proposed *CrossGET* is orthogonal to the existing multimodal Transformer acceleration approaches. And the difference is that *CrossGET* achieves acceleration by reducing the number of tokens while the existing approaches are by shrinking model parameters.

Parameter-efficient Tuning Parameter-efficient tuning aims to reduce the number of learnable parameters while tuning. It includes adapters [19, 58], prompt tuning [36, 28], low-rank adaptation [20, 22], parameter sharing [34, 52], dropout [8, 53] and their combinations [15, 25]. The similarity between them and *CrossGET* is that all of them are all in pursuit of efficiency. And the differences are that they pursue efficiency during training but not for accelerating inference, while *CrossGET* pursue efficiency during inference and accordingly the model inference can be significantly accelerated.

3 Methodology

3.1 Overview

As illustrated in Figure 1, *CrossGET* accelerates vision-language Transformers by ensembling tokens. It can be inserted into the middle of the Self-Attention and Feed Forward Net (FFN) of Transformer layers in both the vision and language branches. To achieve more reliable token-matching, *CrossGET* designs a parallelizable *complete-graph soft matching* (Section 3.2). To achieve the goal of effectively exploiting cross-modal information, *CrossGET* proposes *cross-guided matching and ensemble* based on cross tokens (Section 3.3 and 3.4).

3.2 Complete-Graph Soft Matching

Problem Formulation The token matching aims to determine which tokens need to be stacked together. Suppose there are $N \in \mathbb{N}^+$ tokens in total, and $r \in \mathbb{N}^+$ ($r < N$) tokens among them should be eliminated (*i.e.*, stacked together with other tokens), then the problem of token matching can be formulated as a discrete optimization problem that is to find a set of token pairs:

$$\mathbf{P} = \{(\mathbf{T}_i, \mathbf{T}_j) \mid 0 \leq i, j \leq N, i \neq j\}, \quad |\mathbf{P}| = r, \quad (1)$$

where \mathbf{T}_i denotes tokens i , and $|\cdot|$ denotes the size of the set, to maximize the objective function

$$S = \sum_{(\mathbf{T}_i, \mathbf{T}_j) \in \mathbf{P}} \mathbb{D}(\mathbf{T}_i, \mathbf{T}_j), \quad (2)$$

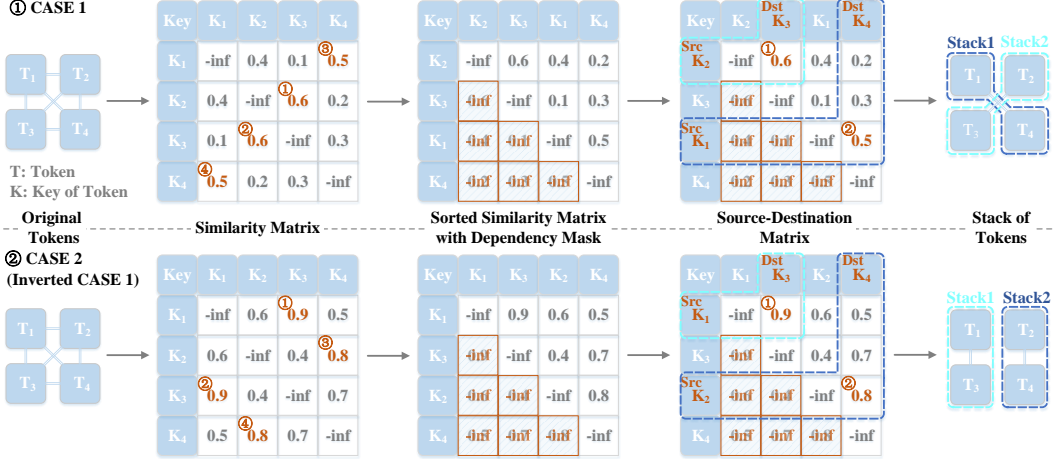


Figure 2: Illustration of complete-graph soft matching on two examples. Case2 is an inverted version of case1 in which the similarity between token pairs in case2 equals $(1 - \text{similarity of corresponding pairs in case1})$.

where \mathbb{D} is a function (e.g., cosine similarity) that calculates the similarity between the key of the token T_i and T_j . For example, when $N = 4$ and $r = 2$, the optimal solution and objective function for two cases shown in Figure 2 are

$$P_1^* = \{(T_1, T_4), (T_2, T_3)\}, \quad S_1^* = \mathbb{D}(T_1, T_4) + \mathbb{D}(T_2, T_3) = 0.5 + 0.6 = 1.1, \quad (3)$$

$$P_2^* = \{(T_1, T_3), (T_2, T_4)\}, \quad S_2^* = \mathbb{D}(T_1, T_3) + \mathbb{D}(T_2, T_4) = 0.9 + 0.8 = 1.7, \quad (4)$$

respectively. Classic clustering-based approaches can be used to obtain the solutions. However, they cannot be parallelized and therefore are time costly. To make token matching parallelizable in mainstream deep learning frameworks (e.g., Pytorch[49]), an additional constraint should be satisfied

$$\mathbf{T}^S = \{T_i \mid (T_i, T_j) \in P\}, \quad |\mathbf{T}^S| = r, \quad (5)$$

$$\mathbf{T}^D = \{T_j \mid (T_i, T_j) \in P\}, \quad |\mathbf{T}^D| \leq r, \quad (6)$$

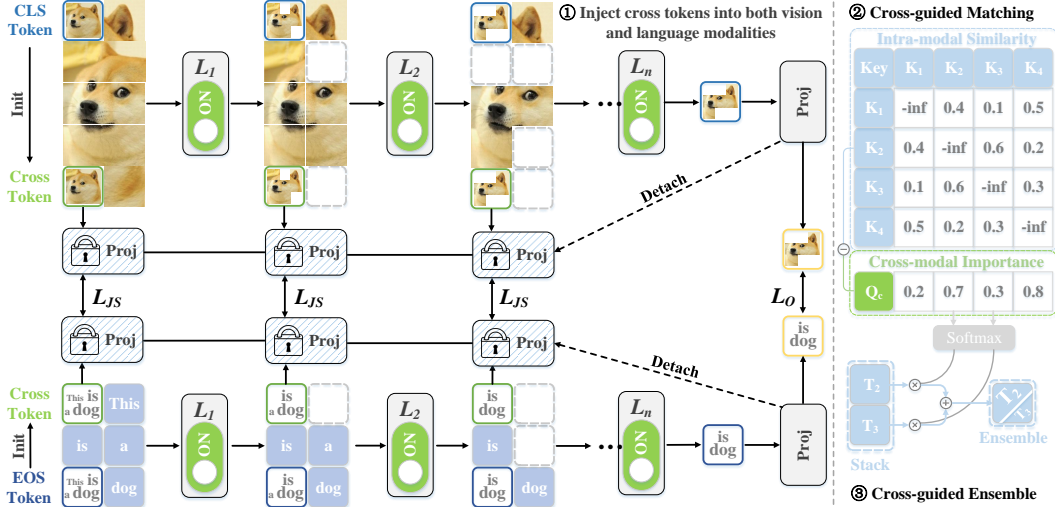
$$\mathbf{T}^S \cap \mathbf{T}^D = \phi, \quad (7)$$

i.e., the set of source tokens \mathbf{T}^S and destination tokens \mathbf{T}^D should be disjointed.

Revisiting Bipartite Soft Matching ToMe [4] suggests a non-iterative *bipartite soft matching* ensure parallelizability which divides tokens into two disjoint sets alternately, for each token in the first set calculates the maximum similarity from it to each token in the other set, and the tokens about the highest similarities will be merged. Take case1 in Figure 2 as an example, tokens are firstly divided into $\{T_1, T_3\}$ and $\{T_2, T_4\}$, then the maximum similarity from T_1 to $\{T_2, T_4\}$ is $\mathbb{D}(T_1, T_4) = 0.5$ and from T_3 to $\{T_2, T_4\}$ is $\mathbb{D}(T_3, T_2) = 0.6$, and the optimal solution is achieved. However for case2, *bipartite soft matching* leads to a worse solution: $P_2^B = \{(T_1, T_2), (T_3, T_4)\} \neq P_2^*$, and $S_2^B = \mathbb{D}(T_1, T_2) + \mathbb{D}(T_3, T_4) = 0.6 + 0.7 = 1.3 < S_2^*$. This is attributed to the design that each token only takes into account the similarity with half but not all other tokens, and the method degrades when tokens with high similarity are not divided into different sets.

Shifting to Complete-Graph Soft Matching A non-iterative complete-graph soft matching is proposed to tackle the above challenge. It enables each token to take into account the similarity with all other tokens as visualized in Figure 2 (a formulated algorithm is provided in the Appendix):

- **Step 1:** For every two tokens, compute the cosine similarities of their keys to get the similarity matrix (self-similarities on the diagonal are set to $-\infty$ and ignored).
- **Step 2:** Sort rows and columns of the similarity matrix in descending order according to their maximum similarity to other tokens.
- **Step 3:** A lower triangle dependency mask is added upon the sorted similarity matrix to help disjoint set \mathbf{T}^S and \mathbf{T}^D . It explicitly prioritizes the matching among tokens by the similarity value, and ensures that source tokens with higher priority will not become targets for other source tokens with lower priority.



- **Step 4:** Pick r rows with the maximum similarity to other tokens as the set of source tokens, and the columns corresponding to other tokens are the sets of destination tokens.
- **Step 5:** Each token in the source set should be stacked together with the token with the highest similarity in the destination set. All five steps are non-iterative and parallelizable.

As shown in Figure 2, *complete-graph soft matching* achieves optimal solutions on both case1 and case2. Due to the space constraint, we provide further discussions on the sub-optimal cases of this method and analyses on how much more similarity information is exploited in the Appendix.

3.3 Cross-Guided Matching

Exploiting Cross-Modal Guidance For multimodal models, in addition to using the intra-modal similarity as guidance introduced above, *complete-graph soft matching* can further benefit from the cross-modal guidance. However, effectively introducing cross-modal guidance is challenging, especially when a dependency exists on the computation order of different modalities.

Intuitively, suppose modality1 needs guidance from modality2 (*e.g.*, to help determine the matching of tokens during inference), then modality2 should conduct inference, and output something provided as cross-modal guidance and send to modality1. However, if there is a computational dependency between modality1 and modality2, *e.g.*, the final output of modality1 is a necessary input for modality2 (BLIP-NLVR [38]), modality2 cannot conduct inference before modality1 finishes its inference, and therefore modality1 is unable to exploit cross-modal guidance provided by modality2.

CrossGET addresses this challenge by decoupling the operation of inference on a modality and the ability to provide guidance for others, *i.e.*, in the previous example, modality2 can provide modality1 guidance without inference. As illustrated in Figure 3, this is achieved by injecting learnable cross tokens into each modality, driving them to learn cross-modal information from each other. When conducting inference within a modality, cross tokens serve as agents for other modalities, providing cross-modal guidance on behalf of other modalities without inference.

Token Matching with Cross-Modal Guidance Cross tokens can provide cross-modal importance as a metric to guide *complete-graph soft matching* further. The cross-modal importance is computed

as the cosine similarity between the query of the cross-token $\mathbf{T}_c \in \mathbb{R}^{1 \times d}$ where d is the embedding size and the key of other tokens $\mathbf{T}_i \in \mathbb{R}^{1 \times d}$, $i \neq c$:

$$I_i = \frac{(\mathbf{T}_c \mathbf{W}^q)(\mathbf{T}_i \mathbf{W}^k)^\top}{\|\mathbf{T}_c \mathbf{W}^q\|_2 \|\mathbf{T}_i \mathbf{W}^k\|_2}, \quad (8)$$

where $\mathbf{W}^q, \mathbf{W}^k \in \mathbb{R}^{d \times d}$ are weights of query and key layers, respectively. $\|\cdot\|_2$ denotes L2-norm. Then *complete-graph soft matching* can further benefit from the cross-modal importance by accordingly changing Step 4 to:

- **Step 4:** Pick r rows with the maximum value of (maximum similarity to other tokens - cross-modal importance) as the set of source tokens, and the columns corresponding to other tokens are the sets of destination tokens.

Loss Function JS divergence [45] (also known as a symmetrized KL divergence [33]) between the projection of cross token T_{cv}^i from vision modality and T_{cl}^i from language modality in layer i is:

$$\mathcal{L}_{\mathcal{J}\mathcal{S}}^i[(\mathbf{T}_{cv}^i \tilde{\mathbf{W}}^v) \| (\mathbf{T}_{cl}^i \tilde{\mathbf{W}}^l)] = \frac{1}{2} \left[\mathcal{L}_{\mathcal{KL}}^i[(\mathbf{T}_{cv}^i \tilde{\mathbf{W}}^v) \| \mathbf{T}_m^i] + \mathcal{L}_{\mathcal{KL}}^i[(\mathbf{T}_{cl}^i \tilde{\mathbf{W}}^l) \| \mathbf{T}_m^i] \right], \quad (9)$$

$$\mathbf{T}_m^i = \frac{1}{2}(\mathbf{T}_{cv}^i \tilde{\mathbf{W}}^v + \mathbf{T}_{cl}^i \tilde{\mathbf{W}}^l), \quad (10)$$

where $\tilde{\mathbf{W}}^v$ and $\tilde{\mathbf{W}}^l$ are the detached weight of the final projection layer in vision modality and language modality, respectively. The detached implies $\mathcal{L}_{\mathcal{J}\mathcal{S}}^i$ only produce gradients with respect to cross tokens \mathbf{T}_{cv}^i and \mathbf{T}_{cl}^i but not to projection layers, and the weight of projection layers \mathbf{W}^v and \mathbf{W}^l are updated only according to the gradients from original loss. $\mathcal{L}_{\mathcal{J}\mathcal{S}}^i$ is added to drive cross tokens to learn cross-modal information from different modalities:

$$\mathcal{L} = \mathcal{L}_{\mathcal{O}} + 10^\alpha \sum_{i=0}^{L-1} \mathcal{L}_{\mathcal{J}\mathcal{S}}^i, \quad (11)$$

where $\mathcal{L}_{\mathcal{O}}$ is the original loss to learn a multimodal model, α is a hyperparameter to keep loss items to have the same order of magnitude, and L is the number of model layers, which means cross tokens are inserted into each layer of the model and $\mathcal{L}_{\mathcal{J}\mathcal{S}}$ should be computed for each layer.

3.4 Cross-Guided Ensemble

After the matching of tokens is finished, a straightforward design to ensemble the stacked tokens is to add them up simply with all the same weights. Benefit from the cross-modal importance metric already used to guide token matching, this design can be further improved by introducing cross-modal guidance into the ensemble, *i.e.*, use the softmax value of cross-modal importance to produce weighted summation of the stacked tokens as the results of the ensemble:

$$\mathbf{T}_i = \sum_{\mathbf{T}_j \in \mathcal{S}_i} \frac{e^{I_j}}{\sum_{\mathbf{T}_k \in \mathcal{S}_i} e^{I_k}} \mathbf{T}_j, \quad (12)$$

where \mathcal{S}_i is the set of the stacked tokens, and \mathbf{T}_i is the corresponding ensembled token.

4 Experiments

We report the performance of *CrossGET* on modality-independent model CLIP [50] as well as modality-dependent model BLIP [38], and understanding tasks such as Image-Text Retrieval as well as generation task such as Image Caption. More experiments are provided in the Appendix.

4.1 Experiments with CLIP on Image-Text Retrieval task

We conduct experiments on the CLIP model, and Flickr30K datasets [68] with Karpathy split [26] of Image-Text Retrieval and Text-Image Retrieval task. The number of tokens is reduced to half with the same reduction number for each layer. For example, suppose one of the modalities of a 12-layer

Table 1: Accelerate CLIP on the Flickr30K dataset of the Image-Text Retrieval task. R: Recall. R@1, R@5 and R@10 are the higher the better. CrossGET[▲] only uses *complete-graph soft matching* (Section 3.2), CrossGET[◆] adds *cross-guided matching* (Section 3.3) on [▲], and CrossGET[★] further adds *cross-guided ensemble* (Section 3.4) on [▲]. Here *UPop*[54] use a larger CLIP as its original model, and therefore GFLOPs is higher.

Approach	Image → Text			Text → Image			GFLOPs	Throughput
	R@1	R@5	R@10	R@1	R@5	R@10		
CLIP [50]	92.1	99.1	99.7	79.3	95.7	98.0	20.6	255.2
UPop. <i>ICML'23</i> [54]	82.9	95.7	97.8	67.3	89.5	93.5	51.3	-
ToMe. <i>ICLR'23</i> [4]	90.8 _{↓1.3}	99.2 _{↑0.1}	99.5 _{↓0.2}	78.1 _{↓1.2}	95.3 _{↓0.4}	97.7 _{↓0.3}	11.8	417.4
CrossGET [▲] (CGSM)	90.9 _{↓1.2}	99.2 _{↑0.1}	99.9 _{↑0.2}	79.1 _{↓0.2}	95.1 _{↓0.6}	97.6 _{↓0.4}	11.9	408.9
CrossGET [◆] (CGM)	92.1 _{↑0.0}	99.3 _{↑0.2}	99.7 _{↑0.0}	79.5 _{↑0.2}	95.3 _{↓0.4}	97.7 _{↓0.3}	12.0	402.1
CrossGET [★] (Ours)	92.1 _{↑0.0}	99.7 _{↑0.6}	99.8 _{↑0.1}	79.6 _{↑0.3}	95.7 _{↑0.0}	98.0 _{↑0.0}	12.0 _{↓42%}	401.8 _{↑57%}

Table 2: Ablation study about *CrossGET* on different modalities. The grey background indicates the best.

Modality	I2T R@1	T2I R@1	GFLOPs
vision only	92.1	79.6	12.0
language only	92.8 _{↑0.7}	80.4 _{↑0.8}	19.3 _{↑61%}
vision and language	91.4 _{↓0.7}	78.3 _{↓1.3}	10.6 _{↓12%}

Table 3: Ablation study about the strategy of adding cross tokens.

Depth	I2T R@1	T2I R@1	GFLOPs
deep	92.1	79.6	12.0
shallow	91.5 _{↓0.6}	79.5 _{↓0.1}	12.0
share	90.7 _{↓1.4}	78.8 _{↓0.8}	12.0

Table 4: Ablation study about initializing cross tokens.

Initialization	I2T R@1	T2I R@1	GFLOPs
[CLS]+[EOS]	92.1	79.6	12.0
zero	91.7 _{↓0.4}	77.9 _{↓1.7}	12.0
normal random	90.4 _{↓1.7}	77.6 _{↓2.0}	12.0
uniform random	90.2 _{↓1.9}	77.6 _{↓2.0}	12.0

Table 5: Ablation study about projection layer detach.

Projection detach	I2T R@1	T2I R@1	GFLOPs
both	92.1	79.6	12.0
vision only	91.4 _{↓0.7}	79.4 _{↓0.2}	12.0
language only	90.5 _{↓1.6}	78.9 _{↓0.7}	12.0
neither	91.5 _{↓0.6}	78.9 _{↓0.7}	12.0

CLIP has 100 tokens as input, then $\lfloor \frac{100}{12} \rfloor = 8$ tokens will be eliminated from each layer so that the number of tokens left in the last layer is $100 - 12 \times 8 = 4$, and the total number of tokens across all layers is roughly reduced to half. If not specified, the number of tokens to be reduced in other experiments is also determined by this strategy. Table 1 demonstrates that *CrossGET* outperforms both the SOTA multimodal model pruning approach *UPop* [54] and SOTA unimodal token reduction approach *ToMe* [54] without extra learnable parameter other than negligible cross tokens³.

4.2 Ablation Studies

Effect of individual components As highlighted by the grey background in Table 1, *complete-graph soft matching* (CGSM) brings improvements on most of the metrics and a significant improvement on text-to-image retrieval (recall@1 increases from 78.1 to 79.1). Since the complete graph have more similarity of token pairs to compute than the bipartite graph, GFLOPs also slightly increases by 0.1. *Cross-guided matching* (CGM) brings further improvement on most metrics and a significant improvement on image-to-text retrieval (recall@1 increases from 90.9 to 92.1). Since cross tokens interact with other tokens during the forward, GFLOPs again slightly increases by 0.1. *Cross-guided ensemble* brings final improvement on all metrics with negligible extra GFLOPs. Compared to the original CLIP, *CrossGET* achieves the same image-to-text recall@1 and 0.3 higher text-to-image recall@1 while saving 42% GFLOPs and improving throughput by 57%.

³For fairness of comparison, token reduction methods that require additional learnable parameters exceeding the level of several tokens are not taken into comparison (e.g., simply adding a new linear projection layer with weight $W \in \mathbb{R}^{768 \times 768}$ already needs 768 times the number of our cross token’s parameters $T_c \in \mathbb{R}^{1 \times 768}$).

Table 6: Accelerate BLIP on the NLVR2 dataset of the Vision Reasoning task. BLIP is the original model for all acceleration approaches.

Approach	Dev Acc	Test Acc	GFLOPs	Throughput
BLIP [38]	82.3	83.4	132.5	39.8
UPop. <i>ICML'23</i> [54]	80.3 \downarrow 2.0	81.1 \downarrow 2.3	89.4	-
ToMe. <i>ICLR'23</i> [4]	81.7 \downarrow 0.6	82.2 \downarrow 1.2	59.0	81.9
CrossGET (Ours)	82.1 \downarrow 0.2	83.2 \downarrow 0.2	61.1 \downarrow 57%	76.8 \uparrow 93%

Table 7: Ablation study about tokens for computing importance.

used tokens	Dev Acc	Test Acc
all tokens	82.1	83.2
cross token	82.1 \uparrow 0.0	82.9 \downarrow 0.3
other tokens	81.9 \downarrow 0.2	82.2 \downarrow 1.0
importance	82.2 \uparrow 0.1	83.0 \downarrow 0.2

Table 8: Accelerate BLIP on the COCO Caption dataset of the Image Caption task. The suffix -F denotes GFLOPs and throughput for the forward, while -G denotes GFLOPs and throughput for the generation.

Approach	CIDEr	SPICE	GFLOPs-F	Throughput-F	GFLOPs-G	Throughput-G
BLIP [38]	133.3	23.8	65.7	106.4	330.7	17.2
UPop. <i>ICML'23</i> [54]	128.9 \downarrow 4.4	23.3 \downarrow 0.5	39.8	-	-	-
ToMe. <i>ICLR'23</i> [4]	130.3 \downarrow 3.0	23.3 \downarrow 0.5	29.2	209.3	43.8	77.7
CrossGET (Ours)	131.6 \downarrow 1.7	23.8 \uparrow 0.0	30.1 \downarrow 54%	183.5 \uparrow 72%	46.7 \downarrow 86%	73.9 \uparrow 330%

Effect on different modalities As shown in Figure 3, it is flexible that *CrossGET* can be applied on both vision and language modalities or only on one of the modalities. Table 2 investigates the trade-off between model performance and computational cost of application on different modalities. Experimental results show that *CrossGET* only on the vision modality achieves the best trade-off.

Effect of cross token depth There are several strategies for injecting cross tokens into the model. For example, (1) deep: adding different cross tokens for each layer; (2) shallow: only adding one cross token into the first layer; (3) share: adding one cross token but jointly optimized in each layer. Table 3 shows that adding different cross tokens for each layer achieves the best performance.

Effect of cross token initialization Cross tokens are sensitive to the initialization strategy. Using the [CLS] token to initialize the cross token in the vision modality and [EOS] token to initialize cross token in the language modality is recommended (for models that do not use the [EOS] token in the language branch, we use the first token of the input tokens to initialize instead). Table 4 shows that zero initialization and random initialization perform worse.

Effect of projection layer detach The final projection layers are initially used for projecting features from the different modalities into aligned representations. In *CrossGET*, the final projection layers are detached from the original model and used for aligning cross tokens. The detach operation prevents gradients with respect to cross tokens from updating the projection layers. Table 4 shows that both detaching vision and language projection give improved performance.

4.3 Experiments with BLIP on the Visual Reasoning task

Table 6 shows *CrossGET* also achieves very competitive performance on the BLIP model and NLVR2 dataset of a vision reasoning task that requires predicting whether a given sentence can describe a pair of given images. Compared to the original BLIP, *CrossGET* gets only 0.2 lower accuracies on the dev set and test set while saving 57% GFLOPs and improving throughput by 93%.

A different setting from default is that not cross tokens alone but all tokens are used to compute importance. By default, only the [CLS] and [EOS] token matter for final outputs, while for BLIP-NLVR, all tokens from the vision modality are the input for the language modality and therefore matters. As shown in Table 7: (1) all tokens (adopted): cross tokens contribute to $\frac{1}{2}$ importance while other tokens contribute to the other $\frac{1}{2}$. (2) cross token: cross tokens contribute all; (3) other tokens: other tokens contribute all; (4) importance: we can reuse the dot product between the query and key of each token (including cross tokens) that has already been calculated in the Self-Attention as the importance metric to avoid extra computational cost for introducing other tokens' importance.

Table 9: Accelerate BLIP on the NoCaps dataset of the Novel Object Caption task. All metrics are the higher the better, and the evaluation uses the same model finetuned on the COCO Caption dataset as in Table 8, and therefore the GFLOPs and throughput of models are the same as in Table 8.

Approach	in-domain		near-domain		out-domain		entire	
	CIDEr	SPICE	CIDEr	SPICE	CIDEr	SPICE	CIDEr	SPICE
BLIP [38]	111.9	14.9	108.8	14.8	112.1	14.2	109.9	14.7
ToMe. <i>ICLR'23</i> [4]	107.9 \downarrow 4.0	14.8 \downarrow 0.1	105.1 \downarrow 3.7	14.4 \downarrow 0.4	106.4 \downarrow 5.7	14.1 \downarrow 0.1	105.7 \downarrow 4.2	14.4 \downarrow 0.3
CrossGET (Ours)	113.2 \uparrow 1.3	15.1 \uparrow 0.2	107.2 \downarrow 1.6	14.6 \downarrow 0.2	107.4 \downarrow 4.7	14.1 \downarrow 0.1	108.1 \downarrow 1.8	14.6 \downarrow 0.1

Table 10: Ablation study about which tokens are used for computing JS divergence as additional loss items.

JS divergence as loss	CIDEr	SPICE	GFLOPs
between cross tokens and all tokens	131.6	23.8	30.1
only between pairs of cross tokens	130.2 \downarrow 1.4	23.7 \downarrow 0.1	30.1
only between cross tokens and other tokens	131.0 \downarrow 0.6	23.5 \downarrow 0.3	30.1
w/o weighting loss according to generation order	131.2 \downarrow 0.4	23.7 \downarrow 0.1	30.1

4.4 Experiments with BLIP on the Image Caption task

For generation tasks such as Image Caption that produces results in an auto-regressive manner, *CrossGET* achieves higher speedups than understanding tasks. As shown in Table 8, reducing the total tokens by half for the generation brings 86% saving of GFLOPs and improving 330% throughput. We also conduct experiments on the NoCaps [1] datasets of the Novel Object Caption task, and the model accelerated by *CrossGET* again achieves superior performances.

A different setting from default is that not only the loss of JS divergence between the pairs of cross tokens but also between the cross tokens and other tokens should be added. By default, in language modality, only the [EOS] token matters for the final output, while for the auto-regressive BLIP-Caption, tokens are generated based on their previous tokens and therefore every token matters. Table 10 shows that combined JS divergence between pairs of cross tokens as well as between cross tokens and other tokens as loss performs best; Besides, weighting the loss between cross tokens and other tokens according to the generation order also helps. The weight for the i -th generated token is $1 - \frac{i}{L}$ where L is the length of the maximum generation length, which means the first generated token is more important than the later ones since they are generated based on former ones.

5 Limitation

Table 2 observes that only reducing the number of tokens in the vision modality achieves a better performance-efficiency trade-off than in both the vision and language modalities. However, this is only validated by vision-language Transformers with relatively light language branch, but not validated by ones with heavy language branch (*e.g.*, super LLMs). And this observation can be reserved since the heavy language branch tends to have more redundancy and may be accelerated with a better performance-efficiency trade-off. Due to the limited computational resources, we have to leave the experiments on vision-language Transformers with super LLMs as future work.

6 Conclusion

This paper proposes *CrossGET* as a universal token ensemble framework for accelerating vision-language Transformers. *CrossGET* can effectively leverage cross-modal guidance to help determine which and how tokens should be ensembled. Moreover, the proposed token matching conducted on the complete graph also provides more reliable token-matching results than the existing approach conducted on the bipartite graph. *CrossGET* can achieve better performance-efficiency trade-offs which are thoroughly validated across various vision-language tasks, datasets, and model architectures.

References

- [1] Harsh Agrawal, Karan Desai, Yufei Wang, Xinlei Chen, Rishabh Jain, Mark Johnson, Dhruv Batra, Devi Parikh, Stefan Lee, and Peter Anderson. nocaps: novel object captioning at scale. In *Proceedings of the IEEE International Conference on Computer Vision*, pages 8948–8957, 2019.
- [2] Jean-Baptiste Alayrac, Jeff Donahue, Pauline Luc, Antoine Miech, Iain Barr, Yana Hasson, Karel Lenc, Arthur Mensch, Katherine Millican, Malcolm Reynolds, et al. Flamingo: a visual language model for few-shot learning. *Advances in Neural Information Processing Systems*, 35:23716–23736, 2022.
- [3] Stanislaw Antol, Aishwarya Agrawal, Jiasen Lu, Margaret Mitchell, Dhruv Batra, C Lawrence Zitnick, and Devi Parikh. Vqa: Visual question answering. In *Proceedings of the IEEE international conference on computer vision*, pages 2425–2433, 2015.
- [4] Daniel Bolya, Cheng-Yang Fu, Xiaoliang Dai, Peizhao Zhang, Christoph Feichtenhofer, and Judy Hoffman. Token merging: Your vit but faster. *arXiv preprint arXiv:2210.09461*, 2022.
- [5] Arnav Chavan, Zhiqiang Shen, Zhuang Liu, Zechun Liu, Kwang-Ting Cheng, and Eric P Xing. Vision transformer slimming: Multi-dimension searching in continuous optimization space. In *Proceedings of the IEEE/CVF Conference on Computer Vision and Pattern Recognition*, pages 4931–4941, 2022.
- [6] Tianlong Chen, Yu Cheng, Zhe Gan, Lu Yuan, Lei Zhang, and Zhangyang Wang. Chasing sparsity in vision transformers: An end-to-end exploration. *Advances in Neural Information Processing Systems*, 34:19974–19988, 2021.
- [7] Ekin D. Cubuk, Barret Zoph, Jonathon Shlens, and Quoc V. Le. Randaugment: Practical automated data augmentation with a reduced search space. In *Proceedings of the IEEE/CVF Conference on Computer Vision and Pattern Recognition (CVPR) Workshops*, June 2020.
- [8] Angela Fan, Edouard Grave, and Armand Joulin. Reducing transformer depth on demand with structured dropout. *arXiv preprint arXiv:1909.11556*, 2019.
- [9] Zhiyuan Fang, Jianfeng Wang, Xiaowei Hu, Lijuan Wang, Yezhou Yang, and Zicheng Liu. Compressing visual-linguistic model via knowledge distillation. In *Proceedings of the IEEE/CVF International Conference on Computer Vision*, pages 1428–1438, 2021.
- [10] Elias Frantar and Dan Alistarh. Optimal brain compression: A framework for accurate post-training quantization and pruning. *arXiv preprint arXiv:2208.11580*, 2022.
- [11] Elias Frantar, Saleh Ashkboos, Torsten Hoefler, and Dan Alistarh. Gptq: Accurate post-training quantization for generative pre-trained transformers, 2023.
- [12] Saurabh Goyal, Anamitra Roy Choudhury, Saurabh Raj, Venkatesan Chakaravarthy, Yogish Sabharwal, and Ashish Verma. Power-bert: Accelerating bert inference via progressive word-vector elimination. In *International Conference on Machine Learning*, pages 3690–3699. PMLR, 2020.
- [13] Yash Goyal, Tejas Khot, Douglas Summers-Stay, Dhruv Batra, and Devi Parikh. Making the v in vqa matter: Elevating the role of image understanding in visual question answering. In *Proceedings of the IEEE conference on computer vision and pattern recognition*, pages 6904–6913, 2017.
- [14] Song Han, Huizi Mao, and William J Dally. Deep compression: Compressing deep neural networks with pruning, trained quantization and huffman coding. *arXiv preprint arXiv:1510.00149*, 2015.
- [15] Junxian He, Chunting Zhou, Xuezhe Ma, Taylor Berg-Kirkpatrick, and Graham Neubig. Towards a unified view of parameter-efficient transfer learning. *arXiv preprint arXiv:2110.04366*, 2021.

- [16] Yihui He, Xiangyu Zhang, and Jian Sun. Channel pruning for accelerating very deep neural networks. In *Proceedings of the IEEE international conference on computer vision*, pages 1389–1397, 2017.
- [17] Geoffrey Hinton, Oriol Vinyals, and Jeff Dean. Distilling the knowledge in a neural network. *arXiv preprint arXiv:1503.02531*, 2015.
- [18] Charles AR Hoare. Quicksort. *The computer journal*, 5(1):10–16, 1962.
- [19] Neil Houlsby, Andrei Giurgiu, Stanislaw Jastrzebski, Bruna Morrone, Quentin De Laroussilhe, Andrea Gesmundo, Mona Attariyan, and Sylvain Gelly. Parameter-efficient transfer learning for nlp. In *International Conference on Machine Learning*, pages 2790–2799. PMLR, 2019.
- [20] Edward J Hu, Yelong Shen, Phillip Wallis, Zeyuan Allen-Zhu, Yuanzhi Li, Shean Wang, Lu Wang, and Weizhu Chen. Lora: Low-rank adaptation of large language models. *arXiv preprint arXiv:2106.09685*, 2021.
- [21] Yan Huang, Wei Wang, and Liang Wang. Instance-aware image and sentence matching with selective multimodal lstm. In *Proceedings of the IEEE Conference on Computer Vision and Pattern Recognition*, pages 2310–2318, 2017.
- [22] Nam Hyeon-Woo, Moon Ye-Bin, and Tae-Hyun Oh. Fedpara: Low-rank hadamard product for communication-efficient federated learning. *arXiv preprint arXiv:2108.06098*, 2021.
- [23] Xu Jia, Efstratios Gavves, Basura Fernando, and Tinne Tuytelaars. Guiding long-short term memory for image caption generation, 2015.
- [24] Xiaoqi Jiao, Yichun Yin, Lifeng Shang, Xin Jiang, Xiao Chen, Linlin Li, Fang Wang, and Qun Liu. Tinybert: Distilling bert for natural language understanding. *arXiv preprint arXiv:1909.10351*, 2019.
- [25] Rabeeh Karimi Mahabadi, James Henderson, and Sebastian Ruder. Compacter: Efficient low-rank hypercomplex adapter layers. *Advances in Neural Information Processing Systems*, 34:1022–1035, 2021.
- [26] Andrej Karpathy and Li Fei-Fei. Deep visual-semantic alignments for generating image descriptions. In *Proceedings of the IEEE conference on computer vision and pattern recognition*, pages 3128–3137, 2015.
- [27] Andrej Karpathy, Armand Joulin, and Li F Fei-Fei. Deep fragment embeddings for bidirectional image sentence mapping. *Advances in neural information processing systems*, 27, 2014.
- [28] Muhammad Uzair Khattak, Hanoona Rasheed, Muhammad Maaz, Salman Khan, and Fahad Shahbaz Khan. Maple: Multi-modal prompt learning. *arXiv preprint arXiv:2210.03117*, 2022.
- [29] Gyuwan Kim and Kyunghyun Cho. Length-adaptive transformer: Train once with length drop, use anytime with search. *arXiv preprint arXiv:2010.07003*, 2020.
- [30] Sehoon Kim, Sheng Shen, David Thorsley, Amir Gholami, Woosuk Kwon, Joseph Hassoun, and Kurt Keutzer. Learned token pruning for transformers. In *Proceedings of the 28th ACM SIGKDD Conference on Knowledge Discovery and Data Mining*, pages 784–794, 2022.
- [31] Wonjae Kim, Bokyung Son, and Ildoo Kim. Vilt: Vision-and-language transformer without convolution or region supervision. In *International Conference on Machine Learning*, pages 5583–5594. PMLR, 2021.
- [32] Ryan Kiros, Ruslan Salakhutdinov, and Richard S Zemel. Unifying visual-semantic embeddings with multimodal neural language models. *arXiv preprint arXiv:1411.2539*, 2014.
- [33] Solomon Kullback and Richard A Leibler. On information and sufficiency. *The annals of mathematical statistics*, 22(1):79–86, 1951.

- [34] Zhenzhong Lan, Mingda Chen, Sebastian Goodman, Kevin Gimpel, Piyush Sharma, and Radu Soricut. Albert: A lite bert for self-supervised learning of language representations. *arXiv preprint arXiv:1909.11942*, 2019.
- [35] Carlos Lassance, Maroua Maachou, Joohee Park, and Stéphane Clinchant. A study on token pruning for colbert. *arXiv preprint arXiv:2112.06540*, 2021.
- [36] Brian Lester, Rami Al-Rfou, and Noah Constant. The power of scale for parameter-efficient prompt tuning. *arXiv preprint arXiv:2104.08691*, 2021.
- [37] Junnan Li, Dongxu Li, Silvio Savarese, and Steven Hoi. Blip-2: Bootstrapping language-image pre-training with frozen image encoders and large language models. *arXiv preprint arXiv:2301.12597*, 2023.
- [38] Junnan Li, Dongxu Li, Caiming Xiong, and Steven Hoi. Blip: Bootstrapping language-image pre-training for unified vision-language understanding and generation. *arXiv preprint arXiv:2201.12086*, 2022.
- [39] Junnan Li, Ramprasaath Selvaraju, Akhilesh Gotmare, Shafiq Joty, Caiming Xiong, and Steven Chu Hong Hoi. Align before fuse: Vision and language representation learning with momentum distillation. *Advances in neural information processing systems*, 34:9694–9705, 2021.
- [40] Xiujun Li, Xi Yin, Chunyuan Li, Pengchuan Zhang, Xiaowei Hu, Lei Zhang, Lijuan Wang, Houdong Hu, Li Dong, Furu Wei, et al. Oscar: Object-semantics aligned pre-training for vision-language tasks. In *European Conference on Computer Vision*, pages 121–137. Springer, 2020.
- [41] Youwei Liang, Chongjian Ge, Zhan Tong, Yibing Song, Jue Wang, and Pengtao Xie. Not all patches are what you need: Expediting vision transformers via token reorganizations. *arXiv preprint arXiv:2202.07800*, 2022.
- [42] Tsung-Yi Lin, Michael Maire, Serge Belongie, James Hays, Pietro Perona, Deva Ramanan, Piotr Dollár, and C Lawrence Zitnick. Microsoft coco: Common objects in context. In *European conference on computer vision*, pages 740–755. Springer, 2014.
- [43] Haotian Liu, Chunyuan Li, Qingyang Wu, and Yong Jae Lee. Visual instruction tuning. *arXiv preprint arXiv:2304.08485*, 2023.
- [44] Ilya Loshchilov and Frank Hutter. Sgdr: Stochastic gradient descent with warm restarts. *arXiv preprint arXiv:1608.03983*, 2016.
- [45] ML Menéndez, JA Pardo, L Pardo, and MC Pardo. The jensen-shannon divergence. *Journal of the Franklin Institute*, 334(2):307–318, 1997.
- [46] Paul Michel, Omer Levy, and Graham Neubig. Are sixteen heads really better than one? *Advances in neural information processing systems*, 32, 2019.
- [47] Paulius Micikevicius, Sharan Narang, Jonah Alben, Gregory Diamos, Erich Elsen, David Garcia, Boris Ginsburg, Michael Houston, Oleksii Kuchaiev, Ganesh Venkatesh, et al. Mixed precision training. *arXiv preprint arXiv:1710.03740*, 2017.
- [48] OpenAI. Gpt-4 technical report, 2023.
- [49] Adam Paszke, Sam Gross, Francisco Massa, Adam Lerer, James Bradbury, Gregory Chanan, Trevor Killeen, Zeming Lin, Natalia Gimelshein, Luca Antiga, et al. Pytorch: An imperative style, high-performance deep learning library. *Advances in neural information processing systems*, 32, 2019.
- [50] Alec Radford, Jong Wook Kim, Chris Hallacy, Aditya Ramesh, Gabriel Goh, Sandhini Agarwal, Girish Sastry, Amanda Askell, Pamela Mishkin, Jack Clark, et al. Learning transferable visual models from natural language supervision. In *International Conference on Machine Learning*, pages 8748–8763. PMLR, 2021.

- [51] Yongming Rao, Wenliang Zhao, Benlin Liu, Jiwen Lu, Jie Zhou, and Cho-Jui Hsieh. Dynamicvit: Efficient vision transformers with dynamic token sparsification. *Advances in neural information processing systems*, 34:13937–13949, 2021.
- [52] Dachuan Shi, Ruiyang Liu, Linmi Tao, Zuoxiang He, and Li Huo. Multi-encoder parse-decoder network for sequential medical image segmentation. In *2021 IEEE international conference on image processing (ICIP)*, pages 31–35. IEEE, 2021.
- [53] Dachuan Shi, Ruiyang Liu, Linmi Tao, and Chun Yuan. Heuristic dropout: An efficient regularization method for medical image segmentation models. In *ICASSP 2022-2022 IEEE International Conference on Acoustics, Speech and Signal Processing (ICASSP)*, pages 1101–1105. IEEE, 2022.
- [54] Dachuan Shi, Chaofan Tao, Ying Jin, Zhendong Yang, Chun Yuan, and Jiaqi Wang. Upop: Unified and progressive pruning for compressing vision-language transformers. *arXiv preprint arXiv:2301.13741*, 2023.
- [55] Amanpreet Singh, Ronghang Hu, Vedanuj Goswami, Guillaume Couairon, Wojciech Galuba, Marcus Rohrbach, and Douwe Kiela. Flava: A foundational language and vision alignment model. In *Proceedings of the IEEE/CVF Conference on Computer Vision and Pattern Recognition*, pages 15638–15650, 2022.
- [56] Xiu Su, Shan You, Jiyang Xie, Mingkai Zheng, Fei Wang, Chen Qian, Changshui Zhang, Xiaogang Wang, and Chang Xu. Vitas: vision transformer architecture search. In *European Conference on Computer Vision*, pages 139–157. Springer, 2022.
- [57] Alane Suhr, Stephanie Zhou, Ally Zhang, Iris Zhang, Huajun Bai, and Yoav Artzi. A corpus for reasoning about natural language grounded in photographs. *arXiv preprint arXiv:1811.00491*, 2018.
- [58] Yi-Lin Sung, Jaemin Cho, and Mohit Bansal. VI-adapter: Parameter-efficient transfer learning for vision-and-language tasks. In *Proceedings of the IEEE/CVF Conference on Computer Vision and Pattern Recognition*, pages 5227–5237, 2022.
- [59] Chaofan Tao, Lu Hou, Wei Zhang, Lifeng Shang, Xin Jiang, Qun Liu, Ping Luo, and Ngai Wong. Compression of generative pre-trained language models via quantization. *arXiv preprint arXiv:2203.10705*, 2022.
- [60] Hugo Touvron, Matthieu Cord, Matthijs Douze, Francisco Massa, Alexandre Sablayrolles, and Hervé Jégou. Training data-efficient image transformers & distillation through attention. In *International Conference on Machine Learning*, pages 10347–10357. PMLR, 2021.
- [61] Oriol Vinyals, Alexander Toshev, Samy Bengio, and Dumitru Erhan. Show and tell: A neural image caption generator. In *Proceedings of the IEEE conference on computer vision and pattern recognition*, pages 3156–3164, 2015.
- [62] Peng Wang, An Yang, Rui Men, Junyang Lin, Shuai Bai, Zhikang Li, Jianxin Ma, Chang Zhou, Jingren Zhou, and Hongxia Yang. Unifying architectures, tasks, and modalities through a simple sequence-to-sequence learning framework. *arXiv preprint arXiv:2202.03052*, 2022.
- [63] Wenhui Wang, Furu Wei, Li Dong, Hangbo Bao, Nan Yang, and Ming Zhou. Minilm: Deep self-attention distillation for task-agnostic compression of pre-trained transformers. *Advances in Neural Information Processing Systems*, 33:5776–5788, 2020.
- [64] Guangxuan Xiao, Ji Lin, Mickael Seznec, Julien Demouth, and Song Han. Smoothquant: Accurate and efficient post-training quantization for large language models. *arXiv preprint arXiv:2211.10438*, 2022.
- [65] Zhendong Yang, Zhe Li, Mingqi Shao, Dachuan Shi, Zehuan Yuan, and Chun Yuan. Masked generative distillation. *arXiv preprint arXiv:2205.01529*, 2022.
- [66] Zichao Yang, Xiaodong He, Jianfeng Gao, Li Deng, and Alex Smola. Stacked attention networks for image question answering. In *Proceedings of the IEEE conference on computer vision and pattern recognition*, pages 21–29, 2016.

- [67] Hongxu Yin, Arash Vahdat, Jose M Alvarez, Arun Mallya, Jan Kautz, and Pavlo Molchanov. A-vit: Adaptive tokens for efficient vision transformer. In *Proceedings of the IEEE/CVF Conference on Computer Vision and Pattern Recognition*, pages 10809–10818, 2022.
- [68] Peter Young, Alice Lai, Micah Hodosh, and Julia Hockenmaier. From image descriptions to visual denotations: New similarity metrics for semantic inference over event descriptions. *Transactions of the Association for Computational Linguistics*, 2:67–78, 2014.
- [69] Jiahui Yu, Zirui Wang, Vijay Vasudevan, Legg Yeung, Mojtaba Seyedhosseini, and Yonghui Wu. Coca: Contrastive captioners are image-text foundation models. *arXiv preprint arXiv:2205.01917*, 2022.
- [70] Zhihang Yuan, Lin Niu, Jiawei Liu, Wenyu Liu, Xinggang Wang, Yuzhang Shang, Guangyu Sun, Qiang Wu, Jiaxiang Wu, and Bingzhe Wu. Rptq: Reorder-based post-training quantization for large language models, 2023.
- [71] Linfeng Zhang, Jiebo Song, Anni Gao, Jingwei Chen, Chenglong Bao, and Kaisheng Ma. Be your own teacher: Improve the performance of convolutional neural networks via self distillation. In *Proceedings of the IEEE/CVF International Conference on Computer Vision*, pages 3713–3722, 2019.
- [72] Mingjian Zhu, Yehui Tang, and Kai Han. Vision transformer pruning. *arXiv preprint arXiv:2104.08500*, 2021.

7 Supplementary Methodology Details

7.1 Algorithm Implementation of Complete-Graph Soft Matching

Algorithm 1: Complete-Graph Soft Matching

Input: Number of tokens N , number of tokens to be reduced r , original tokens $\mathbf{T} = \{\mathbf{T}_i\}_{i=1}^N$ and their corresponding keys $\mathbf{K} = \{\mathbf{K}_i\}_{i=1}^N$ where $|\mathbf{T}| = |\mathbf{K}| = N$

Output: Reduced tokens $\mathbf{T}^* = \{\mathbf{T}_i^*\}_{i=1}^{N-r}$ where $|\mathbf{T}^*| = N - r$

- 1 # Step1: Calculate the cosine distance D_{ij} between the keys of tokens
- 2 $\mathbf{D} = \frac{\mathbf{K}\mathbf{K}^\top}{\|\mathbf{K}\|_2^2} + \text{diag}(\underbrace{-\infty, -\infty, \dots, -\infty}_N)$, $\mathbf{D} \in \mathbb{R}^{N \times N}$, $\text{diag} : \mathbb{R}^N \rightarrow \mathbb{R}^{N \times N}$
- 3 # Step2: Descendingly sort similarity matrix \mathbf{D} by maximum similarity
- 4 $\mathbf{A}^S = \text{argsort}(\max_{1 \leq j \leq N} D_{ij}) \in \mathbb{R}^N$, $\mathbf{A}^D = \text{argsort}(\max_{1 \leq i \leq N} D_{ij}) \in \mathbb{R}^N$
- 5 $\mathbf{D}^* = \text{sort}_d(\text{sort}_s(\mathbf{D}, \mathbf{A}^S), \mathbf{A}^D)$, $\text{sort}_s : D_{ij}^* \leftarrow D_{\mathbf{A}_i^S j}$, $\text{sort}_d : D_{ij}^* \leftarrow D_{i \mathbf{A}_j^D}$
- 6 # Step3: Add a lower triangle dependency mask \mathbf{M}
- 7 $\mathbf{D}^* = \mathbf{D}^* + \mathbf{M}$, $M_{ij} = \begin{cases} -\infty & \text{for } i \geq j \\ 0 & \text{for } i < j \end{cases}$
- 8 # Step4: Pick source tokens \mathbf{T}^S and destination tokens \mathbf{T}^D by similarity
- 9 $\mathbf{A} = \text{argsort}(\max_{1 \leq j \leq N} D_{ij}^*) \in \mathbb{R}^N$, $\mathbf{A}^S = (\mathbf{A}_i)_{1 \leq i \leq r} \in \mathbb{R}^r$, $\mathbf{T}^S = \{\mathbf{T}_i | i \in \mathbf{A}^S\}$
- 10 $\mathbf{A} = \underset{j \in (\{k\}_{k=1}^N \setminus \mathbf{A}^S)}{\text{argmax}} D_{ij}^* \in \mathbb{R}^N$, $\mathbf{A}^D = (\mathbf{A}_i)_{i \in \mathbf{A}^S} \in \mathbb{R}^r$, $\mathbf{T}^D = \{\mathbf{T}_i | i \in \mathbf{A}^D\}$
- 11 # Step5: Average source and corresponding destination tokens
- 12 **return** $\mathbf{T}^* = [\mathbf{T} \setminus (\mathbf{T}^S \cup \mathbf{T}^D)] \cup \{\frac{1}{2}(\mathbf{T}_i^S + \mathbf{T}_i^D)\}_{i=1}^r$

Algorithm 1 is the detailed implementation of the proposed *complete-graph soft matching*. The Step1 ~ 5 in the comments of Algorithm 1 correspond to the Step1 ~ 5 described in Section 3.2 of the main text. Moreover, algorithm 1 is similar to ToMe [4] in terms of parallelizability that there are no sequential loops, and therefore data can be processed in parallel within each step by parallelizable operations (such as *bmm*, *matmul*, *scatter* and *gather* in Pytorch [49]).

7.2 Algorithm Implementation of Cross-Guided Matching and Ensemble

Algorithm 2: Cross-Guided Matching and Ensemble (improvements upon Algorithm 1)

Input: Same inputs as Algorithm 1, **plus query of the cross token \mathbf{Q}**

Output: Same as Algorithm 1

- 1 # Step1~3: Same as Algorithm 1
- 2 # **Step4:** Pick source and destination tokens by similarity **and importance**
- 3 $\mathbf{I} = \frac{\mathbf{K}\mathbf{Q}^\top}{\|\mathbf{K}\|_2 \|\mathbf{Q}\|_2} \in \mathbb{R}^N$
- 4 $\mathbf{A} = \text{argsort}(\max_{1 \leq j \leq N} D_{ij}^* - \mathbf{I}) \in \mathbb{R}^N$, $\mathbf{A}^S = (\mathbf{A}_i)_{1 \leq i \leq r} \in \mathbb{R}^r$, $\mathbf{T}^S = \{\mathbf{T}_i | i \in \mathbf{A}^S\}$
- 5 $\mathbf{A} = \underset{j \in (\{k\}_{k=1}^N \setminus \mathbf{A}^S)}{\text{argmax}} D_{ij}^* \in \mathbb{R}^N$, $\mathbf{A}^D = (\mathbf{A}_i)_{i \in \mathbf{A}^S} \in \mathbb{R}^r$, $\mathbf{T}^D = \{\mathbf{T}_i | i \in \mathbf{A}^D\}$
- 6 # **Step5:** **Sum weighted** source and corresponding destination tokens
- 7 $\mathbf{P} = \{(\mathbf{T}_i^S, \mathbf{T}_i^D)\}_{i=1}^r$, $\mathbf{W} = \{\text{softmax}(\mathbf{I}_i, \mathbf{I}_j) | (\mathbf{T}_i, \mathbf{T}_j) \in \mathbf{P}\}$
- 8 **return** $\mathbf{T}^* = [\mathbf{T} \setminus (\mathbf{T}^S \cup \mathbf{T}^D)] \cup \{\sum_{j=1}^{|\mathbf{W}_i|} \mathbf{W}_{ij} \mathbf{P}_{ij}\}_{i=1}^r$

Algorithm 2 demonstrates how to improve *complete-graph soft matching* by adding *cross-guided matching and ensemble* upon it. It is worth noting that line7 ~ 8 in Algorithm 2 does not imply that only two tokens are in each stack of tokens to be ensemble. This is because different source tokens in \mathbf{T}^S may have the same destination token in \mathbf{T}^D , which implies that the size of the stack is allowed

to be larger than two (in this case, the procedure of ensembling stacks with the different number of tokens can still be implemented by parallelizable operations such as *scatter_add* in Pytorch[49]).

7.3 Sub-optimal Cases for Complete-Graph Soft Matching

Section 3.2 has already shown the cases that *complete-graph soft matching* achieves optimal matching, and here we provide more analyses on the sub-optimal cases of *complete-graph soft matching*.

The main sub-optimal cases come from the trade-off between parallelizability and matching accuracy. To achieve parallelizability, the set of source token T^S and destination tokens T^D have to be disjoint:

$$T^S \cap T^D = \phi. \quad (13)$$

Otherwise, consider

$$T^S \cap T^D = \{T_x\} \neq \phi, \quad 1 \leq x \leq N \quad (14)$$

where N is the number of the original tokens, then

$$(\exists T_i \in T^S \text{ s.t. } (T_i, T_x) \in P) \wedge (\exists T_j \in T^D \text{ s.t. } (T_x, T_j) \in P) \quad (15)$$

where $P = \{(T_i^S, T_i^D)\}_{i=1}^r$ is the set of the paired tokens to be ensembled, is true. However, there is a computational dependency between merging T_i into T_x and merging T_x into T_j . The two operations of the merging require iterations and therefore cannot be parallelized.

T^S and T^D are disjoint (*i.e.*, Equation 13 holds) is equivalent to the constraint

$$\forall T_i \in T^S, T_i \notin T^D \quad (16)$$

is satisfied. In the Step1 of the Algorithm 1, computation is conducted on a complete graph. Therefore T^S and T^D are joint, and constraint 16 does not been satisfied. In Step3, the added lower triangle dependency mask ensures that source tokens with higher priority (*i.e.*, whose keys have higher maximum cosine similarity to keys of other tokens) will not become targets for other source tokens with lower priority, *i.e.*, a relaxed constraint

$$\forall T_i \in T^S, T_i \notin (T_j^D)_{i \leq j \leq N} \quad (17)$$

is satisfied. However, the unsatisfied part of the constraint 16

$$\forall T_i \in T^S, T_i \notin (T_j^D)_{1 \leq j < i} \quad (18)$$

indicates that source tokens with low priority may still become targets for other source tokens with high priority. To further satisfy constraint 18, the line10 of Step4 in Algorithm 1 explicitly removes all elements of the source token set from the set of all tokens to construct the set of the destination tokens. And the sub-optimal cases for *complete-graph soft matching* arise when

$$\operatorname{argmax}_{j \in (\{k\}_{k=1}^N \setminus A^S)} D_{ij}^* \neq \operatorname{argmax}_{j \in \{k\}_{k=1}^N} D_{ij}^*, \quad (19)$$

which indicates a source token may exist whose closest destination token in T^D happens to be another source token in T^S . For parallelizability, this destination token is removed from T^D , resulting in the source token can only match the second closest destination token in the set of reduced T^D .

7.4 Expectation of Optimal Matching Probability and Complexity Analysis

Expectation of Optimal Matching Probability For a token $T_i \in T$, assume that any other token $T_j \in T \setminus \{T_i\}$ has the same probability of being its optimal destination token, *i.e.*

$$\forall 1 \leq j \leq N, \quad p((K_i, K_j) = \operatorname{argmax}_{\substack{1 \leq k \leq N \\ k \neq i}} s(K_i, K_k)) = \frac{1}{N-1} \quad (20)$$

where $s(x, y)$ is a function that calculates cosine similarity between x and y .

For *complete-graph soft matching*, in layer l ($1 \leq l \leq L$), suppose $X \sim p(x)$ is a discrete random variable about whether a token from T^S ($|T^S| = r$) can find its optimal destination token in T^D

($|\mathbf{T}^D| = N - lr$), and the probability distribution $p(x)$ is:

$$p(\mathbf{X} = \text{can}) = \sum_1^{|\mathbf{T}^D|} p((\mathbf{K}_i, \mathbf{K}_j)) = \underset{\substack{1 \leq k \leq N+(1-l)r \\ k \neq i}}{\text{argmax}} s(\mathbf{K}_i, \mathbf{K}_k) \quad (21)$$

$$= \frac{N - lr}{N + (1-l)r - 1}. \quad (22)$$

$$p(\mathbf{X} = \text{not}) = 1 - p(\mathbf{X} = \text{can}). \quad (23)$$

Denote $\mathbf{L} \sim p(l)$ as a discrete random variable ($\mathbf{L} \perp\!\!\!\perp \mathbf{X}$) about the current layer number, and

$$\forall 1 \leq l \leq L, \quad p(\mathbf{L} = l) = \frac{1}{L} \quad (24)$$

Denote $h(\mathbf{X}, \mathbf{L})$ as a indicator function

$$h(\mathbf{X}, \mathbf{L}) = \begin{cases} 1 & \text{for } \mathbf{X} = \text{can} \\ 0 & \text{for } \mathbf{X} = \text{not} \end{cases} \quad (25)$$

Then the expectation of a token from \mathbf{T}^S can find its optimal destination token in \mathbf{T}^D is

$$\mathbb{E}^C = \mathbb{E}_{\mathbf{X}\mathbf{L}} [h(\mathbf{X}, \mathbf{L})] = \sum_{l \in \mathbf{L}} \sum_{x \in \mathbf{X}} h(x, l) p_{\mathbf{X}\mathbf{L}}(x, l) \quad (26)$$

$$= \sum_{l \in \mathbf{L}} \sum_{x \in \mathbf{X}} h(x, l) p_{\mathbf{X}}(x) p_{\mathbf{L}}(l) \quad (27)$$

$$= \sum_{l=1}^L [1 \cdot p(\mathbf{X} = \text{can}) + 0 \cdot p(\mathbf{X} = \text{not})] \frac{1}{L} \quad (28)$$

$$= \frac{1}{L} \sum_{l=1}^L \frac{N - lr}{N + (1-l)r - 1} \quad (29)$$

Similarly, given by *bipartite soft matching* used in ToMe [4], the expectation of a token from \mathbf{T}^S ($|\mathbf{T}^S| = \lceil \frac{N+(1-l)r}{2} \rceil$) can find its optimal destination token in \mathbf{T}^D ($|\mathbf{T}^D| = \lfloor \frac{N+(1-l)r}{2} \rfloor$) is

$$\mathbb{E}^B = \frac{1}{L} \sum_{l=1}^L \frac{1}{N + (1-l)r - 1} \lfloor \frac{N + (1-l)r}{2} \rfloor \quad (30)$$

Compare \mathbb{E}^C given by *complete-graph soft matching* with \mathbb{E}^B give by *bipartite soft matching*:

$$\mathbb{E}^C - \mathbb{E}^B = \frac{1}{L} \sum_{l=1}^L \frac{1}{N + (1-l)r - 1} (N - lr - \lfloor \frac{N + (1-l)r}{2} \rfloor) \quad (31)$$

$$\geq \frac{1}{L} \sum_{l=1}^L \frac{1}{N + (1-l)r - 1} (N - lr - \frac{N + (1-l)r}{2}) \quad (32)$$

$$= \frac{1}{L} \underbrace{\left[\sum_{l=1}^{L-1} \frac{1}{N + (1-l)r - 1} \frac{N - lr - r}{2} \right]}_{\text{Part1: } 1 \leq l \leq L-1} + \underbrace{\left[\frac{1}{N + (1-L)r - 1} \frac{N - Lr - r}{2} \right]}_{\text{Part2: } l=L} \quad (33)$$

For part1 in Equation 33, since the number of remaining tokens is always a positive integer, we have

$$N - Lr \geq 1, \quad (34)$$

and therefore for $1 \leq l \leq L - 1$:

$$N - lr \geq r + 1 \Leftrightarrow N - lr - r \geq 1 > 0 \quad (35)$$

always holds. Moreover

$$N + (1 - l)r - 1 = (N - lr - 1) + r > 0 \quad (36)$$

always holds. Furthermore, we have $\text{part1} > 0$ always holds, which indicates the expectation given by *complete-graph soft matching* is higher than *bipartite soft matching* except for the last layer.

For part2 in Equation 33, *bipartite soft matching* evenly divides tokens into two disjoint sets, and the size of each set is not less than r . However, the remaining tokens before the last layer may be less than $2r$. In such a situation, *bipartite soft matching* have to reduce the r to the r^* such that

$$N - Lr^* = r^* \quad (37)$$

complete-graph soft matching follows the same design, and therefore $\text{part2} = 0$ holds. Overall, we have

$$\mathbb{E}^C - \mathbb{E}^B > 0 \quad (38)$$

always holds. For example, for a CLIP [50] model with

$$N = 197, L = 12, r = 16 \quad (39)$$

used in our experiments, given by *complete-graph soft matching*, the expectation of optimal matching probability for a token from T^S is

$$\mathbb{E}^C = \frac{1}{12} \sum_{l=1}^{12} \frac{197 - l \times 16}{197 + (1 - l) \times 16 - 1} \approx 0.78, \quad (40)$$

while given by *bipartite soft matching*, the corresponding expectation is

$$\mathbb{E}^B = \frac{1}{12} \sum_{l=1}^{12} \frac{1}{197 + (1 - l) \times 16 - 1} \lfloor \frac{197 + (1 - l) \times 16}{2} \rfloor = 0.50 < \mathbb{E}^C \quad (41)$$

Complexity Analysis Since the *sort* and *argsort* operations in Algorithm 1 and 2 can be solved by algorithms with $\mathcal{O}(N \log N)$ complexity such as *QuickSort* [18], the major complexity $\mathcal{O}(N^2)$ comes from the computation of cosine similarities between each pair of tokens.

A comparison of different matching methods is listed in Table 11, which demonstrates that as a parallelizable method, *CrossGET* can achieve relatively high expectation of optimal matching probability for a certain token from T^S with relatively low complexity.

Table 11: A comparison of different matching methods. Denote N as the number of the original tokens, r as the number of tokens to be reduced, and T as the number of iterations for k-means.

Method	Iterative	Parallelizable	Expectation of Optimal Matching Probability	Complexity
greedy search	Yes	✗	1	$\mathcal{O}(rN^2)$
k-means	Yes	✗	≤ 1	$\mathcal{O}(rNT)$
random	No	✓	$\frac{1}{N-1} \approx 0$	$\mathcal{O}(r)$
ToMe [4]	No	✓	$\frac{1}{L} \sum_{l=1}^L \frac{1}{N+(1-l)r-1} \lfloor \frac{N+(1-l)r}{2} \rfloor \approx 0.5$	$\mathcal{O}(N^2)$
CrossGET (Ours)	No	✓	$0.5 < \frac{1}{L} \sum_{l=1}^L \frac{N-lr}{N+(1-l)r-1} \leq 1$	$\mathcal{O}(N^2)$

7.5 Diagram of Adding Cross Tokens to CLIP and BLIP

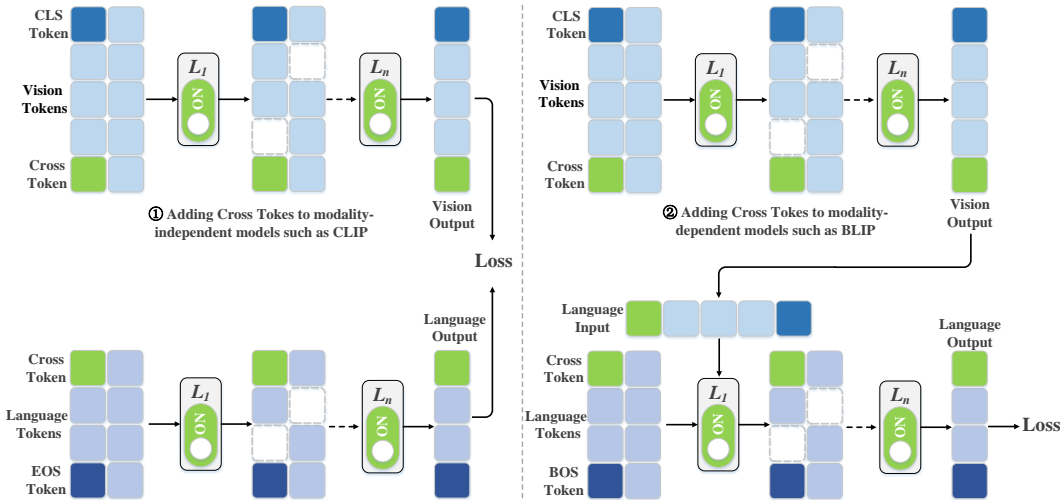


Figure 4: Diagram of adding cross tokens to modality-independent models such as CLIP [50] (left) and modality-dependent models such as BLIP [38] (right).

Figure 4 demonstrates that *CrossGET* is designed to be a universal framework that can be used for accelerating both modality-independent and modality-dependent vision-language models.

8 Supplementary Experiments and Details

8.1 Hyperparameter Settings

Table 12: Training hyperparameters for accelerating various vision-language models, tasks, and datasets.

Hyperparameters	CLIP-Retrieval [50]	BLIP-NLVR [38]	BLIP-Caption [38]		BLIP-VQA [38]
	Flickr30K [68]	NLVR2 [57]	COCO [42]	NoCaps [1]	VQAv2 [13]
Optimizer	AdamW				
AdamW β	(0.9, 0.999)				
Batch size	512				
Weight decay	0.2	0.05	0.05	0.05	0.05
Epochs	12	15	5	5	10
Initial learning rate	1e-5	3e-6	1e-5	1e-5	2e-5
Learning rate schedule	CosineLRScheduler [44]				
Data augmentation	RandomAugment [7]				
Training Precision	Mixed Precision [47]				
Matching loss coefficient	10^0	10^1	10^2	10^2	10^1
Required GPUs	$8 \times V100$	$8 \times V100$	$8 \times A100$	$8 \times A100$	$8 \times A100$

Table 13: Structure hyperparameters for all models used in our experiments. Superscript * indicates 2 Transformers share parameters.

Model	Input resolution	Vision Transformer				Language Transformer			
		number	layers	width	heads	number	layers	width	heads
CLIP-Retrieval	336×336	1	12	768	12	1	12	512	8
BLIP-NLVR	384×384	2*	12	768	12	1	12	768	12
BLIP-Caption	384×384	1	12	768	12	1	12	768	12
BLIP-VQA	480×480	1	12	768	12	2	12	768	12

8.2 Experiments with BLIP on the Visual Question Answer task

Table 14: Accelerate BLIP on the VQA2.0 dataset of the Visual Question Answer task. "yes/no", "number", "other", and "overall" denote accuracy on the corresponding types of questions. These four metrics are the higher the better. The superscript ^F denotes GFLOPs and throughput for the forward that a single image may be accompanied by multiple questions and answers during training. And the superscript ^T denotes GFLOPs and throughput for the test that a single image is accompanied by only one question and answer.

Approach	yes/no	number	other	overall	GFLOPs ^F	Throughput ^F	GFLOPs ^T	Throughput ^T
BLIP [38]	92.6	60.6	68.3	77.4	186.1	67.2	106.8	53.0
UPop. <i>ICML'23</i> [54]	-	-	-	76.3 \downarrow 1.1	109.4	-	-	-
ToMe. <i>ICLR'23</i> [4]	92.1 \downarrow 0.5	59.3 \downarrow 1.3	67.1 \downarrow 1.2	76.5 \downarrow 0.9	119.0	141.1	46.7	90.1
CrossGET (Ours)	92.4 \downarrow 0.2	59.7 \downarrow 0.9	67.7 \downarrow 0.6	77.0 \downarrow 0.4	124.5 \downarrow 33%	120.4 \uparrow 79%	49.0 \downarrow 54%	81.3 \uparrow 53%

We conduct experiments on the BLIP model [38] and the test-dev set of the VQA2.0 dataset [13]. Table 14 demonstrates that *CrossGET* can also considerably save computational cost and improve throughput for the Visual Question Answer task. For example, compared to the original model, *CrossGET* gets only 0.4 lower overall accuracy on all three types of questions while saving 33% GFLOPs and improving throughput by 79% for the multiple-question scenario, and saving 54% GFLOPs and improving throughput by 53% for the single-question scenario.